Journal of Atmospheric and Solar-Terrestrial Physics 80 (2012) 239–246

Contents lists available at SciVerse ScienceDirect

Journal of Atmospheric and Solar-Terrestrial Physics

journal homepage: www.elsevier.com/locate/jastp

Study of post sunset vertical plasma drift at equatorial F-region using long-term (1990–2003) ionosonde measurements in Indian longitude

B. Kakad [a,*], D. Tiwari [a], T.K. Pant [b]

[a] Indian Institute of Geomagnetism, Plot No. 5, Sector-18, New Panvel 410218, Maharashtra, India
[b] Space Physics Laboratory, VSSC, Thiruvananthapuram 695022, India

A R T I C L E I N F O

Article history:
Received 30 September 2011
Received in revised form
28 January 2012
Accepted 5 February 2012
Available online 15 February 2012

Keywords:
Equatorial ionosphere
F-region vertical drift
Ionosonde

A B S T R A C T

Ionosonde measurements from Trivandrum (77°E, 8.5°N, dip 0.5°N) are used to investigate the seasonal and solar flux dependence of peak height, and vertical drift of F layer in post sunset hours. The study reveals that pre- and post-reversal peak vertical drift of F layer increases with solar flux in all seasons. However, the rate of increase is found to be season dependent. Clear difference is observed in the solar flux dependence of peak height and vertical drift for two equinoxes. The post reversal peak westward electric field shows weak (strong) dependence on solar flux during November–February solstice (March–April, September–October equinox).

1. Introduction

Earth's magnetic field and ambient electric field plays an important role in the dynamics of equatorial ionosphere. Many interesting phenomena like equatorial ionization anomaly (EIA), equatorial electrojet (EEJ), pre-reversal enhancement (PRE), equatorial spread F (ESF) are observed at the equatorial ionosphere, which results from complex interaction between E- and F-region dynamo electric fields. Equatorial ionospheric zonal electric field is eastward during the day and turns westward during the night time. This eastward electric field enhances rapidly in the post sunset hours before turning to westward, which is termed as pre-reversal enhancement (PRE). As a result, equatorial F layer moves upward under the influence of $\mathbf{E}\times\mathbf{B}$ force and comes down at later time when PRE eastward electric field dies down. Theoretical models have shown that PRE is mainly caused due to F-region dynamo (Rishbeth, 1971; Heelis et al., 1974; Farley et al., 1986). Recently, the relation between duskside F-region dynamo current density and PRE is established by satellite observations by Park et al. (2010).

Extensive study of zonal and vertical plasma drifts has been carried out using incoherent scatter radar measurement from equatorial station Jicamarca (Fejer et al., 1985, 1989, 1991). Ionosonde and HF doppler radar data are also utilized to investigate the vertical plasma drifts in Indian longitude (Namboothiri et al., 1989; Goel et al., 1990; Subbarao and Krishna Murthy, 1994; Hari and Krishna Murthy, 1995; Ramesh and Sastri, 1995; Prabhakaran Nayar and Sreehari, 2004; Abdu et al., 2010; Mathew et al., 2010). Vertical plasma drifts estimated using different techniques are compared and found to be in good agreement with drift observations at Jicamarca (Fejer et al., 1995; Oyekola, 2006; Woodman et al., 2006; Oyekola et al., 2008). These investigations have shown that the height of F layer, zonal and vertical plasma drift vary considerably from day-to-day, season-to-season, with solar flux and magnetic activity. Study using satellite observations has shown that zonal plasma drift changes considerably with altitude (Coley and Heelis, 1989). Recently, the longitudinal variation of equatorial vertical ion drift at the topside ionosphere is examined using DMSP satellite data (Hartman and Heelis, 2007). Theoretical and numerical simulation studies have provided the additional tool to investigate the longitudinal and seasonal variation of plasma drifts (Fesen et al., 2000; Richmond et al., 2003; Vichare and Richmond, 2005).

Study of F-region height, zonal and vertical plasma drift with LT, altitude, longitude, season and solar flux using long-term data is of great interest as this information provides the input for the global thermospheric and ionospheric models and hence helps to understand the dynamics of the equatorial ionosphere (Heelis et al., 1990; Scherliess and Fejer, 1999; Fejer et al., 2005; Fejer et al., 2008; Yue et al., 2008). Studies have also reported that post sunset height of the F layer plays an important role in the occurrence of ESF irregularities (Farley et al., 1970; Abdu et al., 1983; Sastri, 1984; Kelley and Maruyama, 1992; Jayachandran et al., 1993; Jyoti et al., 2004). However, in many studies March–April and September–October equinoxes are not investigated separately. Also much attention is not given to downward

* Corresponding author. Tel.: +91 22 27484203; fax: +91 22 27480762.
E-mail address: bkakad9@gmail.com (B. Kakad).

1364-6826/$ - see front matter © 2012 Elsevier Ltd. All rights reserved.
doi:10.1016/j.jastp.2012.02.004

movement of F layer in post-reversal hours. Thus present work is carried out to investigate the seasonal and solar flux dependence of peak height, pre- and post-reversal peak vertical drift of F layer in post sunset hours using long-term (1990–2003) ionosonde measurements from Trivandrum. Zonal electric fields are computed using magnetic field data recorded at the same station. The data analysis technique is described in Section 2. Details of correction applied to apparent vertical drift estimated below 300 km are provided in Section 3. Results are discussed in Section 4 and present work is summarized in Section 5.

2. Data used and methodology

In the present study, ionosonde data recorded at Trivandrum (77°E, 8.5°N, dip 0.5°N) for the period of January 1993–February 2003 is used, together with data for the March–April equinox during 1990–1992. Altogether 126 months data are available during 1990–2003. The virtual height of the F layer base, h′F is scaled manually from 00 to 24LT for each nth day of a month. Here, 24LT implies the 00LT of $n+1$th day. It should be noted that h′F is not scaled when the base of F layer is not clearly visible in the ionogram due to occurrence of strong range or frequency spread F. Generally, periods with three hourly geomagnetic activity index $ap \geq 18$ or days with daily geomagnetic activity index $Ap \geq 18$ are considered as magnetically disturbed. For a given day, $Ap = \Sigma ap(i)/8$ corresponds to average magnetic activity during 00–24UT hours, where $i = 1,2..8$. In the present study, LT variation of post sunset base height of F layer is considered, hence a new index Ap' is calculated as: $Ap'_n = 1/8[ap_{n-1}(7)+ap_{n-1}(8)+\Sigma ap_n(i)]$ where $i = 1,2..6$, for each nth day. Ap' represents the average magnetic activity between ~00 and 24LT hours for a given day. Here, days with $Ap' < 18$ are considered as magnetically quiet. Sometimes the effect of magnetic activity is seen on following day as well due to the disturbance dynamo (Scherliess and Fejer, 1997; Fuller-Rowell et al., 2002; Fejer et al., 2005; Kakad et al., 2007). Hence to assure that observed variation of h′F reflects only the quiet time pattern, it is made sure that the previous day of each quiet day under consideration is also magnetically quiet.

A monthly quiet time average of h′F ($\langle h'F \rangle$) is obtained by taking 15 min average from 17 to 31LT for magnetically quiet days of a month. Here, 31LT implies 07LT of following day. Monthly average is estimated only if data are available for more than two quiet days and there are 116 such months, which satisfies this condition. Fig. 1 shows the variation of h′F for quiet days superimposed with their monthly average as a function of IST for March, October, December and May during different solar flux conditions. LT for the site of observation, i.e. Trivandrum is given by LT=IST–0.36 h. The average of 10.7 cm solar flux, $\langle S_a \rangle$, is estimated by considering the quiet days with h′F data for that month. The upward movement of h′F resulted from enhanced eastward electric field in post sunset hours is clearly seen for the months shown in Fig. 1a–j. Whereas, for May 1998, and May 1995 (Fig. 1k–l) clear signature of PRE is not observed. Moreover peak in monthly average h′F is seen in post midnight hours for these 2 months. There are 31 such months that do not show a development of PRE in the post sunset hours, which are listed in Table 1. It is noticed that this tendency is mostly seen in the May–August (MJJA) solstice during low to moderate and June–July (JJ) during high solar flux.

The months that show clear increase in $\langle h'F \rangle$ in the post sunset hours due to enhanced eastward electric field are chosen for the present investigation. There are 85 such months and for

Table 1
Provides the list of months in which pre-reversal enhancement (PRE) is absent, with their average solar flux.

Year	Month	Average solar flux
1993	May, June, July	110, 106, 101
1994	May, June, July, August	86, 82, 79, 78
1995	April, May, June, July, August	85, 78, 79, 79, 78
1996	January, June, July, August	74, 72, 73, 75
1997	May, June, July, August	77, 74, 74, 79
1998	May, June, July	121, 112, 116
1999	May, June, July	150, 169, 161
2000	June, July	182, 187
2001	June, July	171, 131
2002	July	175

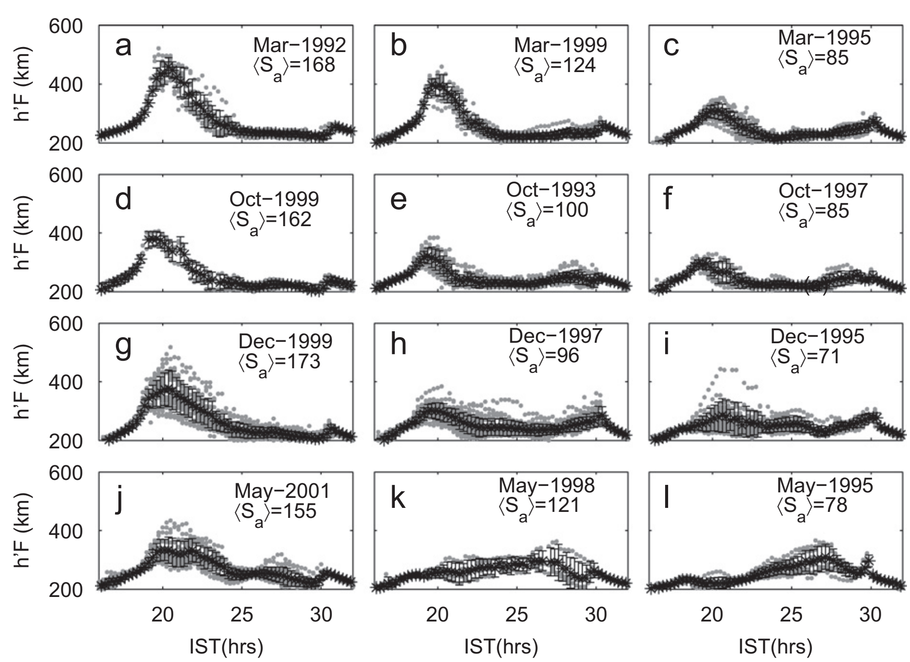

Fig. 1. Monthly quiet time variation of h′F (gray color) superimposed with their average (black color) is shown as a function of IST for March, October, December and May during different solar flux conditions. LT=IST–0.36 h.

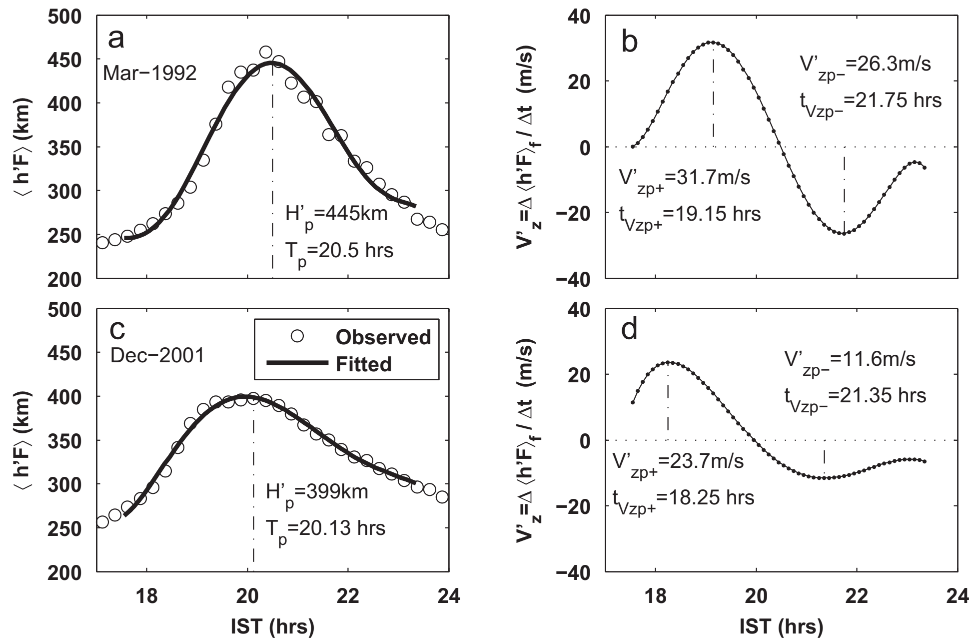

Fig. 2. Monthly quiet time average of observed h′F (empty circles) along with its sixth-order polynomial fit (continuous line) is shown in left vertical panel and their first time derivative in right vertical panel as a function of IST for March 1992 and December 2001.

each month $\langle h'F \rangle$ between 17 and 24IST is fitted with sixth-order polynomial. Monthly average h′F and its sixth-order polynomial fit ($\langle h'F \rangle_f$) is shown as a function of IST in Fig. 2a,c for March 1992 and December 2001, respectively, with their first time derivative in Fig. 2b,d. The error in sixth-order polynomial fitting of $\langle h'F \rangle$ is ≤ 12 km for all 85 months. Peak average virtual height H'_p, peak apparent upward V'_{zp+} and downward drift V'_{zp-} with their time of occurrence namely; T_p, t_{Vzp+} and t_{Vzp-} are computed for each month. The average virtual height at the time of maximum upward (h_{Vzp+}) and downward (h_{Vzp-}) drift of F layer are also estimated. Above mentioned parameters are estimated using monthly quiet time average of apparent base height of F layer and thus gives the information about its quiet time behavior for that month. It should be noted that estimated vertical drift (V'_z) represents apparent vertical drift of base of F layer in the post sunset hours and found to be different for March 1992 and December 2001 (see Fig. 2). In December 2001 downward movement of F layer is slow compared to March 1992. There are 21, 20, 34 and 10 months that fall under March–April (MA), September–October (SO), November–February (NDJF) and May–August (MJJA) seasons, respectively.

3. Corrections to apparent vertical drift

Apparent vertical drift estimated using h′F measurements deviate considerably from true vertical $\mathbf{E} \times \mathbf{B}$ drift during early and late evening hours due to effects of chemical recombination. It should be noted that eastward electric field and recombination at the bottom side of F layer both contribute to apparent upward movement of equatorial F layer in the post sunset hours. Studies have shown that apparent vertical drift estimated above 300 km are close to real vertical drift as the chemical loss on vertical drift is negligible at these altitudes (Bittencourt and Abdu, 1981; Krishna Murthy et al., 1990). Hence the apparent V'_{zp+} and V'_{zp-} obtained from first time derivative of $\langle h'F \rangle_f$ are close to true vertical drift only if they are estimated at an altitude >300 km. Fig. 3 depicts time of occurrence of H'_p, V'_{zp+}, V'_{zp-} and virtual height h_{Vzp+}, h_{Vzp-} for MA, SO, NDJF. Less number of months is available in MJJA season, as PRE is absent on most of the months of this season during low to moderate solar flux. It should be noted that h_{Vzp+} and h_{Vzp-} are <300 km for ~ 40 months. Hence, the maximum pre- and post-reversal vertical drifts (i.e. V_{zp+} and V_{zp-}) estimated below 300 km are corrected for chemical decay of F layer.

True vertical drift can be estimated from apparent vertical drift using relation: $V = V' - \beta H$, where β is chemical loss coefficient and H is electron density scale height. The chemical loss coefficient is given by $\beta = k_1 n[O_2] + k_2 n[N_2]$, where k_1 and k_2 are reaction rates (Rishbeth, 1986). $n[O_2]$ and $n[N_2]$ represent number density of O_2 and N_2 molecules, respectively, and following two reactions are considered for chemical recombination:

$$O^+ + O_2 \rightarrow^{k_1} O_2^+ + O \tag{1}$$

$$O^+ + N_2 \rightarrow^{k_2} NO^+ + N \tag{2}$$

Reaction rates are given by: $k_1 = 2 \times 10^{-11} \times (T_n/300)^{-0.5}$ and $k_2 = 7 \times 10^{-13}$, in units of cm^3/s, which are taken from the study by Anderson and Rusch (1980). Neutral temperature T_n and number densities of O_2 and N_2 molecules are retrieved from MSIS-E-90, which is the revised version of MSIS-86 empirical atmosphere model (Hedin, 1987). This model is available at http://omniweb.gsfc.nasa.gov/vitmo/msis_vitmo.html. Electron density scale height is given by $H = (1/N \times \partial N/\partial h)^{-1}$, where N is the electron density and h is the height. Hari and Krishna Murthy (1995) estimated H using virtual height obtained from ionosonde at two frequencies: 2.5 MHz and 3 MHz and found that H is ~ 10 km. These authors also noticed that the error in $\partial N/\partial h$ obtained from virtual heights instead of true heights is less than 5%. In the study by Hedin et al. (1996) and Mathew et al. (2010) a constant value of $H = 10$ km is used to calculate the correction to apparent vertical drifts. In the present study H is computed using virtual height measurements for two frequencies between ~ 2 MHz and 3 MHz, and estimated H is found to be $4 \leq H \leq 18$ km for all 85 months under consideration. It should be noted that V' represents average apparent vertical drift for a given month, however here, value of H is estimated for a single quiet day of corresponding month and used in the calculations.

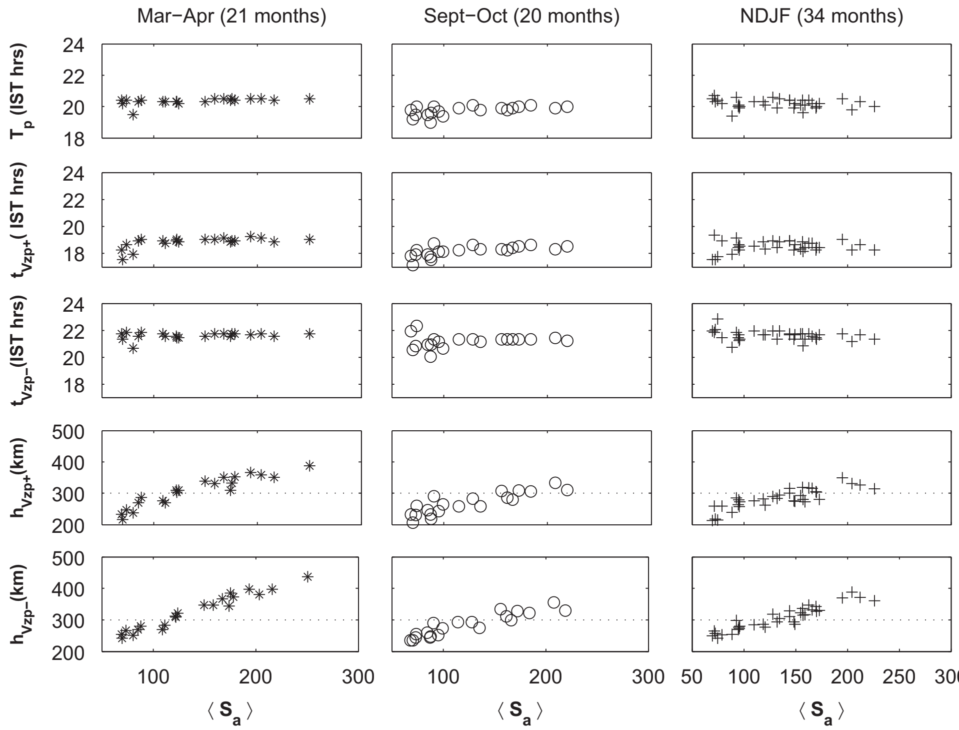

Fig. 3. Time of peak virtual height (T_p), time and height associated with occurrence of maximum apparent upward (i.e. t_{Vzp+}, h_{Vzp+}) and downward drift (i.e. t_{Vzp-}, h_{Vzp-}) are shown as a function of monthly average 10.7 cm solar flux, $\langle S_a \rangle$ for March–April, September–October and November–February seasons in left, middle and right vertical panel, respectively.

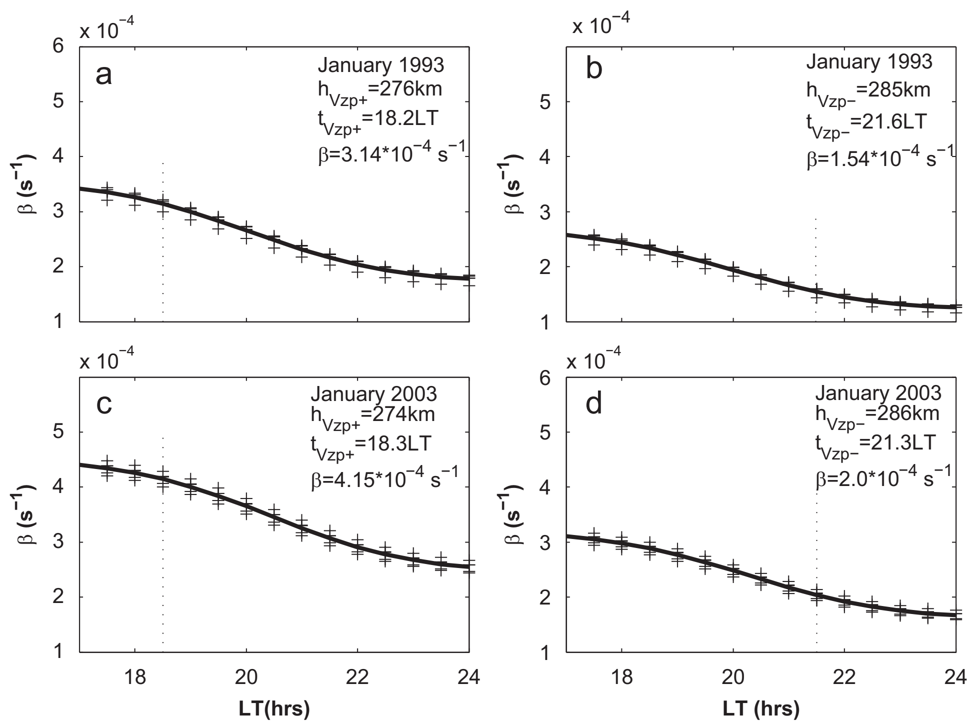

Fig. 4. LT variation of β for five quiet days at an altitude of (a,c) h_{Vzp+} and (b,d) h_{Vzp-} for January 1993 and January 2003. Vertical dotted line represents the time (a,c) t_{Vzp+} and (b,c) t_{Vzp-} for respective month.

MSIS-E-90 model is run for five quiet days of January 1993 and 2003 to get the LT variation of T_n, $n[O_2]$ and $n[N_2]$ at an altitude of h_{Vzp+} and h_{Vzp-} of corresponding months. Chemical loss coefficient β is computed for these 5 days and its LT variation is shown in Fig. 4a,b (c,d) for January 1993 (January 2003). Continuous line indicates the average β for five quiet days of each month. The values of h_{Vzp+} and h_{Vzp-} are mentioned in respective subplots and associated time is shown by vertical dotted line in Fig. 4. It is observed that β has higher values close to sunset period and it decreases significantly at later time. Moreover the day-to-day variability in β is not very high for these months. Thus, β is computed from parameters retrieved from MSIS-E-90 atmospheric model for a single quiet day and used in the calculation. βH estimated at time of t_{Vzp+} and t_{Vzp-} are shown as a function of h_{Vzp+} and h_{Vzp-} in Fig. 5a,b, respectively. It should be noted that βH attains higher values when virtual average height is less than $\sim$ 225 km during 18–20IST. However, for most of the months βH for V'_{zp+}((V'_{zp-}) is found to be <8 m/s (5 m/s). It should be noted that the correction βH applied to V'_{zp+} and V'_{zp-} is less than 25% for all data point considered here.

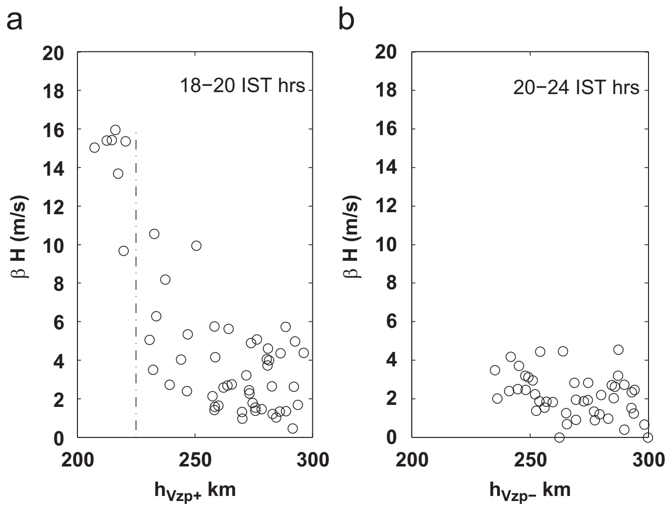

Fig. 5. Chemical loss correction for vertical drifts (βH) is plotted as a function of height at the time of (a) V'_{zp+} and (b) V'_{zp-}.

4. Results and discussion

Fig. 6 depicts monthly maximum (i) average apparent height, (ii) true vertical upward drift, and (iii) true vertical downward drift as a function of average solar flux for MA, SO and NDJF in left, middle and right panel, respectively. H'_p, V_{zp+} and V_{zp-} represent the average values for a month and found to increase with solar flux for all three seasons. However, the rate of increase is different for different seasons. The equations obtained from least square fitting (LSF) of these parameters are given in Table 2 for MA, SO and NDJF.

The correlation coefficient, R, between H'_p, V_{zp+}, V_{zp-} and average solar flux is ≥ 0.75 for all seasons except for the V_{zp-} during NDJF, where correlation is weak. It should be noted that V_{zp+} represents maximum vertical upward drift of F layer in post

Table 2
Empirical relations of H'_p, V_{zp+}, V_{zp-} with average solar flux are summarized with corresponding number of months, correlation coefficient and error in least square fit for MA, SO and NDJF.

Season	Parameter	No. of months (N)	Corr. coeff. (R)	Error in LSF (σ_f)	Equation
MA	H'_p	21	0.96	22.8	$H'_p = 1.46 * \langle S_a \rangle + 174$
	V_{zp+}	18	0.92	3.63	$V_{zp+} = 0.18 * \langle S_a \rangle - 2.86$
	V_{zp-}	18	0.75	4.89	$V_{zp-} = 0.12 * \langle S_a \rangle + 3.0$
SO	H'_p	20	0.90	24.7	$H'_p = 1.10 * \langle S_a \rangle + 192$
	V_{zp+}	13	0.84	3.0	$V_{zp+} = 0.11 * \langle S_a \rangle + 6.85$
	V_{zp-}	14	0.86	2.31	$V_{zp-} = 0.09 * \langle S_a \rangle + 3.62$
NDJF	H'_p	34	0.90	21.0	$H'_p = 1.00 * \langle S_a \rangle + 207$
	V_{zp+}	28	0.84	3.48	$V_{zp+} = 0.13 * \langle S_a \rangle - 0.3$
	V_{zp-}	29	0.30	4.0	–

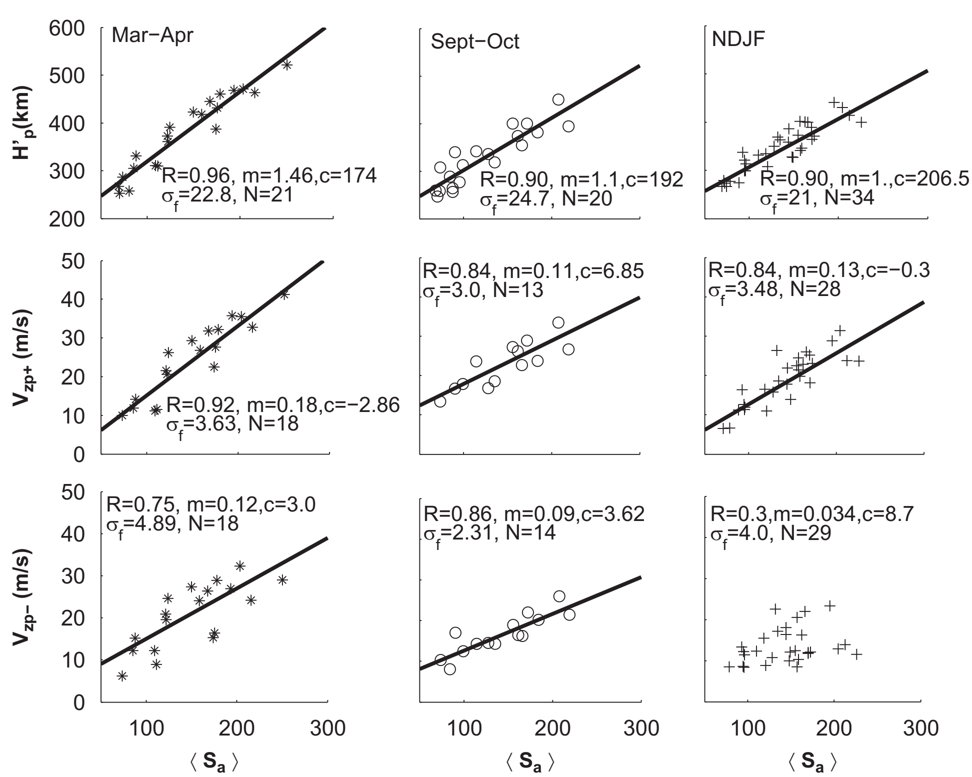

Fig. 6. Monthly average maximum (i) virtual base height, (ii) true upward drift, (iii) true downward drift of F layer are shown as a function of average solar flux, $\langle S_a \rangle$ for three seasons namely; March–April, September–October and NDJF in left, middle and right vertical panel, respectively.

sunset hours and associated with PRE eastward electric field. Whereas, V_{zp-} represents maximum vertical downward drift of F layer and associated with peak background westward electric field when PRE linked eastward electric field dies down. Empirical relations provided in Table 2 suggests that upward and downward movement of F layer in post sunset hours is faster during periods of high solar flux as compared to low solar flux for equinoctial months. However, during NDJF solstice downward movement of F layer is found to be slow even during periods of high solar flux, which results in poor correlation between V_{zp-} and $\langle S_a \rangle$. For MA, SO and NDJF, the pre- and post-reversal peak vertical drifts are ≤ 40 m/s and 30 m/s, respectively.

Influence of solar flux on V_{zp+} and V_{zp-} is found to be considerably different for MA and SO equinox. Fejer et al. (1991) have shown that Jicamarca pre-reversal peak velocity during equinox (MA+SO) varies linearly with solar flux and governed by relation; $V_{zp+} = 0.29 * \langle S_a \rangle - 4.65$. Pre-reversal peak vertical drifts estimated using empirical relation given in Table 2 for MA and SO are lower as compared to estimates of V_{zp+} at Jicamarca. It should be noted that the background magnetic field at F-region height of Jicamarca ($\approx 2.3 \times 10^{-5}$ nT) is lower as compared to Trivandrum ($\approx 3.4 \times 10^{-5}$ nT). Therefore, the values of vertical plasma drift ($\mathbf{V} = \mathbf{E}_{zonal} \times \mathbf{B}_0 / B_0^2$) at Jicamarca are expected to be higher as compared to that at Trivandrum. Fejer et al. (1991) have considered MA and SO together for equinoctial period, but here MA and SO equinoxes are studied separately. It is noticed that the MA and SO equinox behaves differently in response to solar flux. The rate of increase of V_{zp+} and V_{zp-} with solar flux is higher for MA than SO. Also Fejer et al. (1991) have observed the saturation in pre-reversal peak velocity for high solar flux during winter (i.e. May–August for Jicamarca). This saturation tendency is not seen at Trivandrum for high solar flux during winter (i.e. NDJF). We could not compute empirical relations for summer solstice (MJJA) due to less data points. Present work is in general agreement with the study of vertical plasma drift at Trivandrum using HF doppler sounder for different seasons by Balachandran et al. (1993).

Further, study reveals that the magnitude of post-reversal peak downward drift, V_{zp-}, is solar flux and season dependent and found to be $< V_{zp+}$ for all seasons. It should be noted that during NDJF the estimated V_{zp-} shows tendency to increase with solar flux but the dependence is weak due to lot of scatter in plot. It indicates that the downward movement of F layer during NDJF solstice is not controlled entirely by solar flux. The rate of increase of V_{zp-} is found to be lower during SO as compared to MA equinox. Hysell and Burcham (2002) suggested that during high solar flux, magnitude of the pre-reversal enhancement of the eastward electric field is large, causing rapid movement of F layer to higher altitudes, but as post-reversal westward electric field is also larger during periods of high solar activity, F layer comes down faster compared to low solar flux periods. Thus, the present work confirms the results obtained by Hysell and Burcham (2002) and indicates the seasonal dependence of post reversal peak downward drifts. The information about seasonal and solar flux dependence of downward movement of equatorial F layer in post-reversal period might be useful to understand the evolution and structuring of ESF irregularities in post sunset hours.

Eastward electric field in the presence of magnetic field, which is nearly horizontal close to the dip equator results in vertical drift of ions and electrons in post sunset hours. The information of magnetic field at ionospheric height at the site of observation is required in order to estimate the zonal electric field from true vertical drifts. Hence, magnetic field data recorded by ground magnetic observatory at Trivandrum and Tirunelveli (8.7°N, 77.8°E, dip latitude 0.6°N) for the period of January 1990–September 2000 and October 2000–February 2003, respectively, is used. These data are available at http://www.wdciig.res.in. It should be noted that magnetic field data are not available from October 2000 for Trivandrum station. Variation of magnetic field recorded by ground observatory is shown in Fig. 7c together with surface (0 km) magnetic

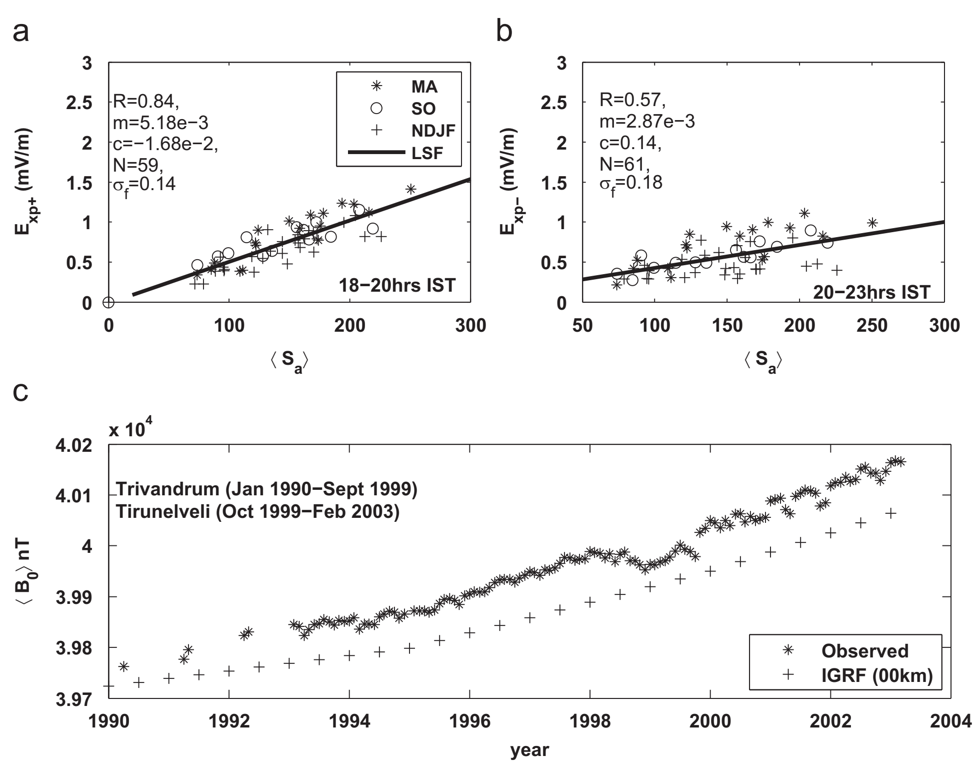

Fig. 7. Maximum (a) pre-reversal eastward and (b) post reversal westward electric field in post sunset hours as a function of average solar flux and (c) monthly average total magnetic field $B_0 = \sqrt{H^2 + Z^2}$ recorded at Trivandrum (January 1990–September 2000) and Tirunelveli (October 2000–February 2003) along with half yearly surface magnetic field at Trivandrum obtained from IGRF model.

field retrieved from IGRF model. This model is available at http://ccmc.gsfc.nasa.gov/cgi-bin/modelweb/models/vitmo_model.cgi. It should be noted that magnetic field obtained from IGRF model is in close agreement with magnetic field data recorded by ground observatory and follows nearly same pattern. Magnetic field obtained from IGRF model at 0 km and 300 km indicates that the surface magnetic field reduces by $\sim 14\%$ at an altitude of 300 km. Hence the magnetic field recorded at Trivandrum is reduced by 14% and used in the calculation of zonal electric field (E_x). The zonal electric field is calculated from true vertical drift using relation: $V_z = E_x/B_0$, where B_0 is magnetic field at F-region heights. Maximum eastward electric field ($E_{xp+} = V_{zp+}/B_0$) and westward electric field ($E_{xp-} = V_{zp-}/B_0$) as a function of average solar flux is shown in Fig. 7a,b, respectively, for MA, SO and NDJF seasons. Empirical relations obtained from LSF for combined data of all the seasons gives: $E_{xp+} = 5.18e{-}3 * \langle S_a \rangle - 0.017$ and $E_{xp-} = 2.878e{-}3 * \langle S_a \rangle + 0.14$. It should be noted that maximum pre-reversal eastward electric field varies with solar flux at higher rate as compared to post-reversal peak westward electric field in post sunset hours.

The present study brings out the difference in development of PRE during MA and SO equinox. Anderson et al. (1982) have reported that total electron content in the equatorial region is significantly different for March and September equinox during high solar flux. These authors found that a change in the neutral composition is mainly responsible for observed differences in ionization during March and September. Recently, Liu et al. (2010) have studied the equinoctial differences in ionospheric electron density during low solar activity period and suggested that neutral winds alone are not enough to explain these observed differences. Recently Sripathi et al. (2011) reported the equinoctial asymmetry in the occurrence of scintillation and ROTI over Indian region. These authors found that height of the F layer is higher during vernal equinox as compared to autumnal equinoxes. Electric and magnetic field plays an important role in the dynamics of equatorial F-region. However, the generation of this electric field is itself controlled by neutral wind, ion neutral collision frequency, E- and F-region conductivities. The seasonal difference observed here in the solar dependence of V_{zp+} and V_{zp-} is mainly attributed to differences in longitudinal gradient of E region conductivity near sunset terminator, sunset time at conjugate points in E-region and background neutral wind (Farley et al., 1986; Tsunoda, 1985; Crain et al., 1993). Thus, the difference in the solar flux dependence of V_{zp+} during MA and SO equinoxes might be associated with the difference in above mentioned parameters during two equinoxes. However, physical mechanism responsible for observed equinoctial asymmetry is still an unanswered question.

5. Summary

In the present study long-term (1990–2003) ionosonde data are utilized from dip equatorial station, Trivandrum in Indian longitude and LT variation of base height of F layer h′F is studied for quiet days of a month in post sunset hours. Solar flux dependence of average peak virtual height (H'_p), true vertical maximum upward (V_{zp+}) and downward drift (V_{zp-}) are investigated for MA, SO and NDJF seasons. Solar flux and season dependence of post sunset peak height and vertical plasma drift of F-region is well known from past many years. The present work is in general agreement with the previous reports of seasonal and solar flux dependence of peak vertical drift in post sunset hours (Fejer et al., 1991, 1995; Fejer et al., 2008; Hari and Krishna Murthy, 1995; Oyekola, 2006).

Many studies have reported that the post sunset height of F-layer plays an important role in the occurrence of EPBs. However, once plasma bubble is developed its evolution might be controlled by background ionospheric conditions. The information on solar flux and season dependence of the post-reversal peak vertical downward drift of F-layer (V_{zp-}) studied here might be useful to understand the evolution and structuring of EPBs during different seasons. Moreover the empirical relations governing the solar flux dependence of H'_p, V_{zp+} and V_{zp-} for different seasons provided in Table 2 may be useful for the related ionospheric studies. Here MJJA season is not studied in detail due to less data points. Some of the main outcomes of present study are listed below:

1. It is found that PRE is absent or rather weak for MJJA(JJ) solstice during low to moderate (high) solar flux.
2. The downward movement of F layer (i.e. V_{zp-}) during NDJF solstice is slower compared to equinoxes and found to be weakly controlled by solar flux.
3. Maximum PRE eastward electric field increases rapidly with average solar flux as compared to post reversal maximum westward electric field.
4. MA and SO equinox behaves differently in response to solar flux and the rate of increase for V_{zp+} and V_{zp-} with $\langle S_a \rangle$ are higher in MA as compared to SO equinox. This may be attributed to differences in neutral wind, background ionospheric conductivities and conductivity gradient near sunset terminator during two equinoxes.
5. The magnitude of V_{zp-} is smaller compared to V_{zp+} for all the seasons.
6. Apparent average peak height H'_p, peak upward V_{zp+} and downward V_{zp-} drift of base of F layer shows tendency to increase with average solar flux and corresponding rate of increase is found to be season dependent, which is in agreement with earlier results.
7. The correction, βH, applied to apparent vertical drift due to chemical decay of F layer is considerably higher at an altitude ≤ 225 km during 18-20IST.

Acknowledgments

We thank WDC, Indian Institute of Geomagnetism for magnetic field data and SPL, VSSC, for ionosonde data. We are also thankful to GSFC, NASA for providing MSISE90 and IGRF models.

References

Abdu, M.A., Medeiros, R.T., Bittencourt, J.A., Batista, S., 1983. Vertical ionization drift velocities and range type spread F in the evening equatorial ionosphere. Journal of Geophysical Research 88, 399.

Abdu, M.A., Batista, I.S., Brum, C.G.M., MacDougall, J.W., Santos, A.M., de Souza, J.R., Sobral, J.H.A., 2010. Solar flux effects on the equatorial evening vertical drift and meridional winds over Brazil: a comparison between observational data and the IRI model and the HWM representations. Advances in Space Research 46, 1078.

Anderson, D.N., Rusch, D.W., 1980. Composition of the nighttime ionospheric F1 region near magnetic equator. Journal of Geophysical Research 85 (A2), 569.

Anderson, D.N., Klobuchar, J.A., DasGupta, A., 1982. Equatorial F-region ionization differences between March and September, 1979. Advances in Space Research 2 (10), 199.

Balachandran, N., Jayachandran, R.B., Rao, P.B., Balan, N., 1993. Seasonal solar and geomagnetic activity effect on F-region vertical plasma drifts. Indian Journal of Radio and Space Physics 22, 89.

Bittencourt, J.A., Abdu, M.A., 1981. A theoretical comparison between apparent and real vertical ionization drift velocities in the equatorial F-region. Journal of Geophysical Research 86, 2451.

Coley, W.R., Heelis, R.A., 1989. Low-latitude zonal and vertical ion drifts seen by DE2. Journal of Geophysical Research 94, 6751.

Crain, D.J., Heelis, R.A., Bailey, G.J., Richmond, A.D., 1993. Low latitude plasma from a simulation of global atmosphere dynamo. Journal of Geophysical Research 98, 6039.

Farley, D.T., Balsley, B.B., Woodman, R.F., Mcclure, J.P., 1970. Equatorial spread F: implications of VHF radar observations. Journal of Geophysical Research 75, 7199.

Farley, D.T., Bonelli, E., Fejer, B.G., Larsen, M.F., 1986. The prereversal enhancement of the zonal electric field in the equatorial ionosphere. Journal of Geophysical Research 91, 13723.

Fejer, B.G., de Paula, E.R., Batista, I.S., Woodman, R.F., 1989. Equatorial F region vertical plasma drifts during solar maxima. Journal of Geophysical Research 94, 12049.

Fejer, B.G., de Paula, E.R., González, S.A., Woodman, R.F., 1991. Average vertical and zonal F region plasma drifts over Jicamarca. Journal of Geophysical Research 96, 13901.

Fejer, B.G., de Paula, E.R., Heelis, R.A., Hanson, W.B., 1995. Global equatorial ionospheric vertical plasma drifts measured by the AE-E satellite. Journal of Geophysical Research 100 (A4), 5769.

Fejer, B.G., Jensen, J.W., Su, S.-Y., 2008. Quiet time equatorial F region vertical plasma drift model derived from ROCSAT-1 observations. Journal of Geophysical Research 113, A05304. doi:10.1029/2007JA012801.

Fejer, B.G., Kudeki, E., Farley, D.T., 1985. Equatorial F region zonal plasma drifts. Journal of Geophysical Research 90, 12249.

Fejer, B.G., Souza, J.R., Santos, A.S., Costa Pereira, A.E., 2005. Climatology of F region zonal plasma drifts over Jicamarca. Journal of Geophysical Research 110, A12310. doi:10.1029/2005JA011324.

Fesen, C.G., Crowley, G., Robel, R.G., Richmond, A.D., Fejer, B.G., 2000. Simulation of pre-reversal enhancement in the low latitude vertical ion drifts. Geophysical Research Letters 27, 1851.

Fuller-Rowell, T.J., Millward, G.H., Richmond, A.D., Codrescu, M.V., 2002. Storm-time changes in the upper atmosphere at low latitudes. Journal of Atmospheric Solar and Terrestrial Physics 64, 1383.

Goel, M.K., Singh, S.S., Rao, B.C.N., 1990. Post-sunset rise of F layer height in the equatorial region and its relation to the F layer dynamo polarization fields. Journal of Geophysical Research 95, 6237.

Hari, S.S., Krishna Murthy, B.V., 1995. Equatorial night-time F-region zonal electric fields. Annals of Geophysics 13, 871.

Hartman, W.A., Heelis, R.A., 2007. Longitudinal variations in the equatorial vertical drift in the topside ionosphere. Journal of Geophysical Research 112, A03305. doi:10.1029/2006JA011773.

Hedin, A.E., 1987. MSIS-86 thermospheric model. Journal of Geophysical Research 92, 4649.

Hedin, A.E., Fleming, E.L., Manson, A.H., Schmidlin, F.J., Avery, S.K., Clark, R.R., Franke, S.J., Fraser, G.J., Tsuda, T., Vial, F., Vincent, R.A., 1996. Empirical wind model for the upper, middle and lower atmosphere. Journal of Atmospheric Solar and Terrestrial Physics 58, 1421.

Heelis, R.A., Hanson, W.B., Bailey, G.J., 1990. Distributions of $He+$ at middle and equatorial latitudes during solar maximum. Journal of Geophysical Research 95, 10313.

Heelis, R.A., Kendall, P.C., Moffet, R.J., Windle, D.W., Rishbeth, H., 1974. Electric coupling of the E and F regions and its effects on F region fields and winds. Planetary and Space Science 22, 743.

Hysell, D.L., Burcham, J.D., 2002. Long term studies of equatorial spread F using the JULIA radar at Jicamarca. Journal of Atmospheric Solar and Terrestrial Physics 64 (12), 1531.

Jayachandran, B., Balan, N., Rao, P.B., Sastri, J.H., Bailey, G.J., 1993. HF Doppler and ionosonde observations on the onset conditions of equatorial spread F. Journal of Geophysical Research 98, 13741.

Jyoti, N., Devasia, C.V., Sridharan, R., Tiwari, D., 2004. Threshold height $(h'F)_c$ for the meridional wind to play a deterministic role in the bottom side equatorial spread F and its dependence on solar activity. Geophysical Research Letters 31, L12809. doi:10.1029/2004GL019455.

Kakad, B., Jeeva, K., Nair, K.U., Bhattacharyya, A., 2007. Magnetic activity linked generation of nighttime equatorial spread F irregularities. Journal of Geophysical Research 112, A07311. doi:10.1029/2006JA012021.

Kelley, M.C., Maruyama, T., 1992. A diagnostic method for equatorial spread F, 2. The effect of magnetic activity. Journal of Geophysical Research 97, 1271.

Krishna Murthy, B., Hari, S., Somayajulu, V., 1990. Nighttime equatorial thermospheric meridional winds from ionospheric h′F data. Journal of Geophysical Research 95 (A4). doi:10.1029/JA095iA04p04307.

Liu, L., He, M., Yue, X., Ning, B., Wan, W., 2010. Ionosphere around equinoxes during low solar activity. Journal of Geophysical Research 115, A09307. doi:10.1029/2010JA015318.

Mathew, T.J., Prabhakaran Nayar, S.R., Ravindran, S., Pant, T.K., 2010. Characteristics of the equatorial F-region vertical plasma drift observed during post-sunset and pre sunrise hours. Advances in Space Research 46, 618.

Namboothiri, S.P., Balan, N., Rao, P.B., 1989. Vertical plasma drifts in the F region at the magnetic equator. Journal of Geophysical Research 94, 12055.

Oyekola, O.S., 2006. Comparison between nighttime ionosonde, incoherent scatter radar, AE-E satellite, and HF Doppler observations of F region vertical electrodynamic plasma drifts in the vicinity of the magnetic equator. Journal of Geophysical Research 111, A11318. doi:10.1029/2006JA011844.

Oyekola, O.S., Ojo, A., Akinrimisi, J., 2008. A comparison of ground and satellite observations of F region vertical velocity near the dip equator. Radio Science 43, RS1005. doi:10.1029/2007RS003699.

Park, J., Luhr, H., Fejer, B.G., Min, K.W., 2010. Duskside F-region dynamo currents: its relationship with pre-reversal enhancement of vertical plasma drift. Annals of Geophysics 28, 2097.

Prabhakaran Nayar, S.R., Sreehari, C.V., 2004. Investigation of height gradient in vertical plasma drift at equatorial ionosphere using multifrequency HF Doppler radar. Journal of Geophysical Research 109, A12308. doi:10.1029/2004JA010641.

Ramesh, K.B., Sastri, J.H., 1995. Solar cycle and seasonal variation in F region vertical drifts over Kodaikanal, India. Annals of Geophysics 19, 633.

Richmond, A.D., Peymirat, C., Roble, R.G., 2003. Long-lasting disturbances in the equatorial ionospheric electric field simulated with a coupled magnetosphere–ionosphere–thermosphere model. Journal of Geophysical Research 108, 1118.

Rishbeth, H., 1971. The F region dynamo. Planetary and Space Science 19, 263.

Rishbeth, H., 1986. On the F2 layer continuity equation. Journal of Atmospheric Solar and Terrestrial Physics 48 (6), 511.

Sastri, J.H., 1984. Duration of equatorial spread F. Annals of Geophysics 2, 353.

Sripathi, S., Kakad, B., Bhattacharyya, A., 2011. Study of equinoctial asymmetry in the Equatorial Spread F ESF irregularities over Indian region using multi-instrument observations in the descending phase of solar cycle-23. Journal of Geophysical Research 116, A11302. doi:10.1029/2011JA016625.

Scherliess, L., Fejer, B.G., 1997. Storm time dependence of equatorial disturbance dynamo zonal electric fields. Journal of Geophysical Research 102, 24037.

Scherliess, L., Fejer, B.G., 1999. Radar and satellite global equatorial F region vertical drift model. Journal of Geophysical Research 104, 6829.

Subbarao, K.S.V., Krishna Murthy, B.V., 1994. Postsunset F-region vertical velocity variation at magnetic equator. Journal of Atmospheric Solar and Terrestrial Physics 56, 59.

Tsunoda, R.T., 1985. Control of the seasonal and longitudinal occurrence of equatorial scintillations by the longitudinal gradient in integrated E-region Pedersen conductivity. Journal of Geophysical Research 90, 447.

Vichare, G., Richmond, A.D., 2005. Simulation study of the longitudinal variation of evening vertical ionospheric drifts at the magnetic equator during equinox. Journal of Geophysical Research 110, A05304. doi:10.1029/2004JA010720.

Woodman, R.F., Chau, J.L., Ilma, R.R., 2006. Comparison of ionosonde and incoherent scatter drift measurements at the magnetic equator. Geophysical Research Letters 33, L01103.

Yue, X., Wan, W., Lei, J., Liu, L., 2008. Modeling the relationship between $E \times B$ vertical drift and the time rate of change of hmF2 $(\Delta hmF2/\Delta t)$ over the magnetic equator. Geophysical Research Letters 35, L05104. doi:10.1029/2007GL033051.